

Hydrothermal synthesis of hydroxyapatite nanorods using a fruit extract template

Maritza Buitrago-Vásquez ^a & Claudia Patricia Ossa-Orozco ^a

^a Grupo de Investigación en Biomateriales, Programa de Bioingeniería, Facultad de Ingeniería, Universidad de Antioquia, Medellín, Colombia.
maritza.buitrago89@gmail.com, claudia.ossa@udea.edu.co

Received: June 20th, 2017. Received in revised form: October 13st, 2017. Accepted: December 15th, 2017.

Abstract

Biocompatible materials development for the replacement of human body parts has been one of the needs of science. Hydroxyapatite is a bioceramic similar to the mineral component present in the human hard tissues and animal body. In this work, hydroxyapatite nanorods were synthesized and characterized using a hydrothermal reaction with templates of fruit extracts in order to control the particles size and morphology. The powders obtained were characterized by scanning electron microscopy, X-ray diffraction, and infrared spectroscopy. Hydroxyapatite nanorods were obtained with diameters between 43.47 and 48.56 nm and lengths between 148.47 and 265.96 nm. For all assays, an adequate HA synthesis was confirmed because the XRD showed the main and secondary peaks. The crystallite size was calculated with the Scherrer equation, obtaining values between 5.99 and 6.96 nm and percentages crystallinity between 55.61 and 65.9%. The synthesized material can be a suitable biomaterial for the manufacture of bone substitutes.

Keywords: hydroxyapatite; bioceramics; nanorods; hydrothermal reaction; fruit extract template.

Síntesis hidrotermal de nanobarras de hidroxiapatita usando plantillas de extractos de fruta

Resumen

El desarrollo de biomateriales para el reemplazo de partes del cuerpo humano ha sido una de las necesidades de la ciencia. La hidroxiapatita es un biocerámico similar al componente mineral de los tejidos duros del cuerpo humano y animal. En la presente investigación, se sintetizaron nanobarras de hidroxiapatita usando síntesis hidrotermal con plantillas de extractos de fruta para controlar el tamaño de partícula. Los polvos obtenidos se caracterizaron por microscopía electrónica de barrido, difracción de rayos x y espectroscopia infrarroja. Las nanobarras obtenidas presentaron diámetros entre 43,47 y 48,56 nm, longitudes entre 148,47 y 265,96 nm. para todos los ensayos los DRX mostraron los picos principales y secundarios de la hidroxiapatita. El tamaño del cristalito fue calculado con la ecuación de Scherrer con valores entre 5,99 y 6,96 nm. y porcentajes de cristalinidad entre 55,61 y 65,9%. En conclusión el material sintetizado puede usarse como biomaterial para aplicaciones óseas.

Palabras clave: hidroxiapatita; biocerámicos, nanobarras; síntesis hidrotermal; plantilla de extracto de fruta.

1. Introduction

The development of new materials to replace parts of the human body, which can be in direct contact with living tissue without causing any damage or condition, has been one of the aims of science during the last couple of decades. Such materials, once proven not to generate adverse reactions with tissues, they have biocompatible characteristic; this

properties are related to the biological acceptance by the body's tissues and they are dependent upon material/tissue interaction, by mechanical stress and by the reaction of degradation generated during implantation. The main use of biocompatible materials is for medical devices that are in direct contact with the human or animal body, such as: prosthesis, pins, osteosynthesis plates, mounting clips/brackets, stents, pacemakers, breast implants, and

How to cite: Buitrago-Vásquez, M. and Ossa-Orozco, P., Hydrothermal synthesis of hydroxyapatite nanorods using a fruit extract template. DYNA, 85(204), pp. 283-288, March, 2018.

elements of stiches, among others [1–3].

Hydroxyapatite (HA) is a biocompatible ceramic, and it is a calcium phosphate similar to the mineral component seen in the hard tissues of the human and animal body, such as bones and teeth, which it is one of the most studied bioceramics. Its chemical formula is $\text{Ca}_{10}(\text{PO}_4)_6(\text{OH})_2$ and stoichiometric ratio Ca/P is equal to 1.67; it can be synthesized by various methods such as solid state reaction, co-precipitation, sol-gel, microemulsion and hydrothermal reaction [1,4].

Current investigations seek to obtain materials that are as similar as possible mechanically and morphologically to the tissues of the human body, specifically the bone, which is constituted mainly by type I collagen fibers and HA nanofibers; morphologically, it has been demonstrated that mineral particles of bone HA are arranged in a matrix embedded in the collagen fibers, due to it, is very important to note the nanoscale [5,6]; having similarity with the before mentioned structure is also important for the enhancement of cell anchorage in biomaterials. The use of templates is one the most flexible, versatile and convenient methods for HA synthesis, since it is very effective for producing particles in nanometric scale, due to the agglomeration degree is minimized and the morphology can be controlled [7]. Recent research has been focused on the use of natural templates, that do not cause environmental effects and minimal changes in the hydroxyapatite chemical composition are generated [7–10].

In this work, HA nanorods were synthesized and characterized using a hydrothermal reaction, which uses high pressures and temperatures above ambient. This method was chosen because it has demonstrated efficacy for obtaining powders in the form of HA fibers with an appropriate crystallinity and stoichiometric Ca/P. Moreover, natural templates of fruit extracts like mango, grape and tamarind were used in order to control the particle size and morphology of the powders obtained.

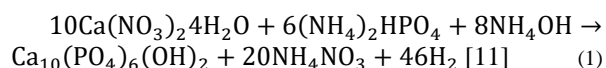
2. Methodology

2.1. Preparation of fruit extracts

The fruit extracts were obtained from locally grown mango, grapes and ripe tamarind. Initially, the fruits were peeled and the seeds were removed, the pulp was washed by being immersed in distilled water, then weighed and macerated in a relation of 10 (w/v) of distilled water from the initial weight. The macerated product was filtered using distillation funnels and filter paper. Then, the resulting filtrate was dried at 40 °C until any excess water had been removed and the product was triturated by hand in a mortar to a fine powder which was used as a template for the HA synthesis [7].

2.2. Hydroxyapatite nanorods synthesis

The nanorods synthesis HA was conducted using the chemical reaction shown in Equation 1:



Calcium nitrate tetrahydrate ($\text{Ca}(\text{NO}_3)_2$) with an 83% purity and ammonium phosphate dibasic ($(\text{NH}_4)_2\text{HPO}_4$) were used as precursors of the reaction, both products of Merck. Distilled water solutions $\text{Ca}(\text{NO}_3)_2$ 0.5 M and $(\text{NH}_4)_2\text{HPO}_4$ 0.3 M (in order to meet the stoichiometric Ca/P = 1.67) were prepared; subsequently the pH was adjusted between 10 to 11, with the addition of ammonium hydroxide. Each fruit extract was added at a rate of 1 wt% ammonium hydroxide to a 0.5 M solution under constant magnetic stirring at 600 rpm; subsequently, a 0.3 M solution of ammonium phosphate dibasic was added drop by drop to a 0.5 M calcium nitrate tetrahydrate solution, with care being taken to maintain an addition of 0.5 ml per minute. The final solution was left to age 12 hours under magnetic stirring at 350 rpm; after this time, it was placed in a sealed teflon autoclave where the hydrothermal reaction was carried out for 24 hours at 180 °C; the vessel was cooled to room temperature and the solution was washed with distilled water and centrifuged at 3000 rpm until reaching a pH at 7. Finally the solution was dried for 24 hours at 60 °C and the obtained powder was stored for further characterization [12–15]. The control sample was called HAC, the sample containing mango extract named HAM, the tamarind sample HAT, and the grape HAG.

2.3. Characterization of hydroxyapatite nanorods

The morphology of the obtained powder was evaluated by Scanning Electron Microscopy SEM, on a microscope JOEL-JSM 6490LV. The information about the material crystallinity and its phases present was analyzed by X-ray diffraction (XRD) using a Rigaku X-ray diffractometer equipped with a source of Cu at an angle of 2θ between 0 ° and 60 ° [16,17]. The crystallite size (D) was obtained by Scherrer-Equation (Equation 2), the percentage crystallinity (% X_c) of the HA powders was calculated using Equation 3. With the objective to provide a quantitative description of the HA nanorods morphology evolution with different fruit template in hydrothermal process, a large number of measurements about length and diameter of HA nanorods were performed directly from the micrographs using the software analysis Image-Processing [7,18,19].

$$D = \frac{0.9\lambda}{\beta \cos\theta} \quad (2)$$

Where $\lambda=1.5418 \text{ \AA}$ is the X-ray wavelength of the Cu radiation, β is the full width at half maximum of the major XDR peak (FWHM) in the plane (2 1 1) and θ is the diffraction angle in the maximum peak [7,18,19].

$$\%X_c = \left(1 - \frac{v_{(112/300)}}{I_{300}}\right) \times 100\% \quad (3)$$

Where $v_{(112/300)}$ is the intensity of the hollow between diffraction peaks of HA in the planes (1 1 2) and (3 0 0) and I_{300} is the intensity of the peak of HA in the plane (3 0 0) [19].

The chemical composition of HA samples were analyzed by an infrared Fourier transform spectroscopy, using a computer model Perkin Elmer Spectrum One DTGS detector.

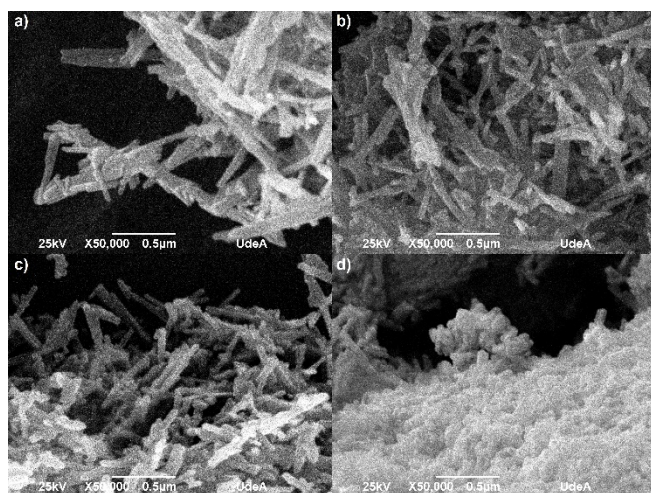


Figure 1. SEM micrographs for different HA powders. a) HAC, b) HAM, c) HAT and d) HAG

Source: The authors.

Table 1.

Sample	Average Length (nm)	Average Diameter (nm)	$D_{(211)}$ (nm)	% X_c
HAC	254.82	43.47	6.26	57.81
HAM	265.96	45.43	5.38	60.27
HAT	222.50	48.56	5.37	55.60
HAG	148.47	43.56	5.37	65.89

Source: The authors.

3. Results and discussion

Figure 1 shows the SEM micrographs for each of the evaluated protocols. In all cases it has been seen that the powders formed agglomerates with elongated particles, common characteristic in nanomaterials due the energy generated between the particles and the superficial area, which increase with the decrease of the particle size [20,21]. The fibers are found on a nanometric scale, the average measures are register in table 1.

In the SEM images observed for all protocols, the morphology are nanorods in the nanometric scale. For HAC (Figure 1a) the obtained fibers had a diameter ranging between 28 and 60 nm and ranging length between 160 and 360 nm; for the HAM (Figure 1b) the fibers had diameters between 28 and 52 nm and lengths between 145 and 400 nm; for HAT (Figure 1c) the obtained fiber diameters ranged between 32 and 65 nm and lengths ranged between 155 and 350 nm; and for HAG (Figure 1d) fiber diameters were between 28 and 55 nm and length were between 100 and 260 nm. In fact, the fibers appear not only embedded in the agglomerate, but also the fiber ends cannot be distinguished clearly. However, while observing the SEM image, it is clear the nanorods that were synthesized with grape extract are smaller and shorter. In the table 1, it has been shown that the variation HA nanorods length is much more substantial than the diameter change with addition of fruit template. The grapes fruit addition reduced the rod length to 41.7% respect HAC, however the HA nanorods diameter remained stable. It

is possible than the fruits particles inhibit the rod, so these were shorter than the control sample.

The HA particles obtained with the fibrous fruits like mango and tamarind have a length value similar to the control HA particles, the amount fiber is 1.6 g per 100 g in the mango and 5.1 g per 100 g in the tamarind, the grape have minor fiber content in the nutritional composition 0.9 g in 100 g. The grape extract, using as template, had a finer appearance, possibly the fiber content of other fruits affected the particle size in each extract obtained in the final milling. It is evident than mango fibers in the fruit have a greater length than tamarind; the mango water content is 83.46% and 31.40% to tamarind, that makes the fibers proportion lower in a specific volume. When elongated particles are milled, it is possible than they begin to slide over each other, this fact can inhibit the milled samples. It is possible than the different characteristics of each fruit extract affect the HA particle obtained, due to these materials can act as inhibitors of the particles growth during the hydrothermal synthesis [22–24].

Given the above data, it can be said that the hydrothermal process yielded the results expected, as fibers were obtained in the nanometers order with or without fruit extracts as template or mold, and this is mainly because during the hydrothermal treatment high pressures and temperatures above 1 atm and 100 °C were employed. The system is closed, inside the dissolution and recrystallization of the material occurs, promoting the formation and stabilization of crystalline phases in the elongated rods form. Nonetheless, it should be clarified that, with regard to crystal growth during hydrothermal treatment and the physico-chemical aspects that occurred during the process, there is still a need to establish complete clarity from a scientific point of view simply because the phenomena that occurred has not been fully defined. Despite this, it can be assumed that the steam generated within the container raises the pressure to the point that this pushes the particles of the reaction against the bottom and edges of the container, and somehow they undergo a type of crushing that gives them an elongated morphology [25,26].

The particles obtained increased in length but not in diameter, which is consistent with Cao et al (2010) who affirm that the formation of nanorods is due to growth of particles in one direction and nanorods may be considered as quasi-one dimensional nanoparticles. These researchers used a polymer for HA synthesis, the polymer was constituted as a growth template, this fact is similar to obtained in this research due to fruit extracts served as a template generating particles in scale nanometric [27].

The surface energy is a parameter than governs the obtained particle shape such as spherical, rod or flat. This energy must be minimal to provide the possibility of having crystals in equilibrium with the surroundings. In natural systems, growth of crystals has typically been thought to occur by atom-by atom addition to an inorganic or organic template or by dissolution of unstable phases (small particles or metastable polymorphs) and reprecipitation of the more stable phase [28]. In the nanoparticles hydrothermal synthesis is necessary to introduce energy to break bonds, to create divisions and generate new surfaces; the driving force existing in the materials during synthesis minimizes the

surface area. Smaller the surface to the volume ratio of the particles, lower the energy state of the material. In order to minimize the surface energy, the directed bonds in isotropic lattices increase crystallization, for example, in rods as it happened in this research [27].

The diffractograms of the nanorods of HA that were obtained by hydrothermal synthesis using fruit extracts as templates (Figure 2) were compared with that reported for the HA pattern (JCPDS 72-1243) [19,29] (Figure 3), in order to determine the correspondence with the main and secondary peaks that characterize the material. For the four powders obtained, that is, HAC, HAM, HAT, and HAG the major peaks are observed at about $2\theta = 31.7^\circ$, 32.2° and 32.9° . While the existence of the secondary peaks are shown at $2\theta = 25.9^\circ$, 34° , 39.7° , 46.7° and 49.4° and the other less intense peaks at $2\theta = 28.88^\circ$ and 53.2° , thus demonstrating that HA was obtained for the four protocols. Notwithstanding, the HAC, HAM and HAT diffractograms have major peaks of dicalcium phosphate anhydrous at about $2\theta = 26.61^\circ$ and 30.18° , and depending on the size of the peaks, it can be estimated that the quantity of this phase is less than 5%. This result corresponds to that specified by ASTM F1185 Standard - 03 (2014), where the chemical standard composition of the hydroxyapatite used in surgical implants is set, indicating that the minimum amount of hydroxyapatite present in these materials must be reported, it is demonstrated and it is natural to be the other 95%. Corroborating this, in some peaks corresponds to other calcium phosphates peaks, as in the case of commercial HA used by Ossa et al (2006) and Gonzalez (2014), in which peaks of tricalcium phosphate appear in their diffractograms [3,30,31].

Table 1 shows the crystallite size calculated with equation 1 in the XRD peak width at half maximum, and has not varied a lot with addition of fruit extracts, however the control sample have a larger crystallite size with respect to other samples, proving that the addition of fruit extract like mango, tamarind and grape decreases in the same proportion the crystallite size.

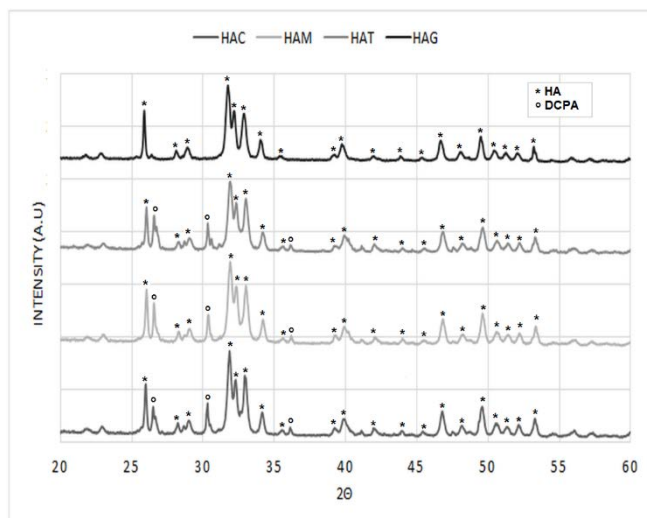


Figure 2. Diffractograms HA powders obtained by hydrothermal synthesis using extract fruits.
Source: The authors.

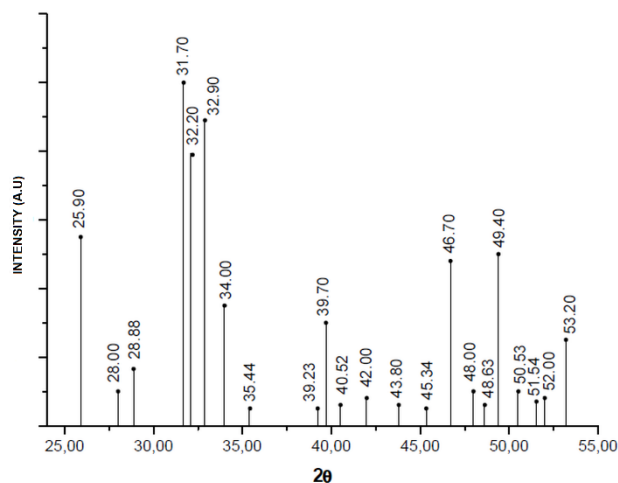


Figure 3. Diffractogram pattern of HA
Source: [29]

The hydroxyapatite percentage crystallinity obtained is presented in Table 1. The hydroxyapatite synthesized with grapes as template has the highest crystallinity percentage with 65.90%. The ASTM F1185-03 (2014) does not provide a guideline about the material crystallinity; on the other hand, some authors suggest that amorphous materials or with low crystallinity are more absorbable, because the physicochemical characteristics such crystallinity and molar ratio Ca/P affect its solubility, protein adsorption and osteoblasts attachment; these may be compromising the cellular material response [30,32,33].

Yang et al. (2015) evaluated the effect of absorption albumin and osteoblasts attachment on hydroxyapatite with different degrees of crystallinity. They found no significant differences between the initial albumin absorption and osteoblasts attachment in HA with crystallinity between 0 and 70%, although for HA with 100% crystallinity, the absorption percentage was reduced. Possibly, the ionic changes interactions that are generated in HA with different crystallinity affect the amount of chemical interactions among calcium ions, due to the fact the ions are readily available to bind electrostatically to proteins. The crystallinity of the synthesized HA in this research was less than 70%, which gives an indication that the manufactured material has optimal characteristics to bind with proteins and precursor cells for new bone formation [34].

Zhou et al (2012) used grape seed polyphenol was used as template for HA synthesis of nanoparticles. They obtained nanoparticles with a diameter of 20-50 nm and poor crystallinity; after thermal treatment at 500°C for 2 hours the crystallinity was increased. On the other hand, Klinkaewnarong et al (2010) used *aloe vera* solution in HA synthesis, they obtained the powder particle sizes among 40–171 nm, the material should has been treated thermally at 500°C to improve the crystallinity and eliminate the Monetite formed with the precursor materials [8,9]. The hydrothermal synthesis method evaluated in this research, provides a possibility to obtain crystalline phases without thermal treatment after synthesis.

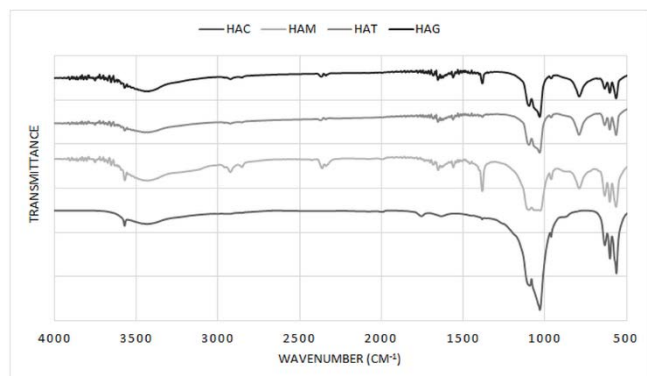


Figure 4. Infrared spectrum of HA powders obtained by hydrothermal synthesis using extract fruits.
Source: The authors.

In Figure 4, the infrared spectrum for HA obtained in the laboratory by means of hydrothermal synthesis is shown for all protocols. A typical HA shows bands at 3578, 3571, 3448 and 633 cm^{-1} characteristic of OH groups; bands at 472, 561, 574, 601, 692, 962, ≈ 1087 1032, 1094, 1040, 1032 cm^{-1} corresponding to bands groups $(\text{PO}_4)_3$; and bands at 870, 1416, 1465, 1480 and 1638 cm^{-1} if the sample contains groups CO_3 [35]. This figure for all protocols shows a suitable composition for HA as bands are observed between 3570.24 and 3572.51, 3427.51 and 3436.04 and 633.68 and 634.58 cm^{-1} corresponding to the OH group, bands approximately in 472.87, between 562.94 and 565.14, 602.06 and 603.72, 962.48 and 962.57, 120.06 and 1031.92 and 1091.5 and 1097.5 cm^{-1} corresponding to $(\text{PO}_4)_3$ groups and bands between 1382.96 and 1384.32 and 1634.66 and 1653 cm^{-1} corresponding to CO_3 groups. Also in the spectrums exist bands approximately in 1045 cm^{-1} corresponding to HA as reported in other studies that synthesized HA with natural agents [7,36–39]. However for the protocols with addition of fruit extract, shows bands unidentified between 2331.94 and 2926.01 cm^{-1} probably corresponding to residues of the fruit extracts used as a natural template for the formation of nanorods, but being a residue of organic and natural type does not affect the final composition of the HA, which is reflected in the XRD where observed a correct stabilization of all phases of this calcium phosphate.

The HA synthesized using the hydrothermal method, regardless of whether it contains or does not contain fruit extracts in its composition, could be an adequate calcium phosphate for use in the manufacture of bone substitutes. This is mainly because the synthesized HA is similar to the mineral component of bones and could be obtained in different-sized nanorods by hydrothermal synthesis, thus allowing a greater similarity to the crystals in the bone [40–42]. Nanosize is considered already minor to 100 nm, particles with this size are used like vector for delivering drugs, growth factors and genetic material. Importantly the size in nanoscale is decisive in the application because the smaller particles can be removed by the kidney, and the larger ones are easier to phagocytose. Recent studies have shown that sizes between 10 and 100 nm are widely distributed in body systems, have shown great impact in terms of cell compatibility, so it is important to further investigate similar

biocompatible materials having the compositions and human body sizes that are within the range of nanoscale [43].

3. Conclusion

Hydroxyapatite nanorods were synthesized using hydrothermal treatment at 180 °C for 24 hours. Adding grape fruit extracts during the synthesis reaction showed that it has a positive effect in the reduction length of particles, the reduction percentage was 41.7 %. It is possible that grapes fiber and water content with relation to mango and tamarind fruit affected the template morphology, this can be done by allowing the length reduction in the nanorods. This is beneficial since it has been shown in some studies that the particle size promotes adequate contact surface to ensure good cell adhesion, especially for different types of bone cells.

Adding the fruit extracts during synthesis hydrothermal of hydroxyapatite nanorods did not affect the phases obtained in the synthesized material, because with or without fruit extract the hydroxyapatite was obtained as the principal phase. Furthermore the crystallinity percentage for all extract fruit evaluated is suitable for possible applications in bone tissue regeneration. On the other hand, the use of fruit extracts is a natural option inside in a synthetic method without affecting the final product. The fruits used are easy to get in Colombia in low cost, in addition, the quantity of fruits extracts used in the hydroxyapatite synthesis process are not much.

Acknowledges

Thanks to the Committee for Development Research, University of Antioquia -CODI- for their funding of the project. To Dayana Meza Terraza Science Laboratory of Surfaces at the University of Antioquia for her help in obtaining images by scanning electron microscopy and, last but not least, to Lina Paola Higueta for facilitating hydrothermal synthesis equipment.

References

- [1] Amor-Márquez, A., Los materiales y su biocompatibilidad: Hidroxiapatita, Mater. Av., 3, pp. 44-48, 2005.
- [2] Park, J. and Lakes, R.S. Biomaterials: an introduction, Thirt, Springer, 2007.
- [3] González-Ocampo, J., Evaluación de las propiedades de cuerpos porosos de hidroxiapatita, obtenidos por gel-casting y su infiltración en espumas poliméricas. Tesis de Maestría, Universidad de Antioquia, Medellín, Colombia, 2013.
- [4] Padmanabhan, S.K., Balakrishnan, A., Chu, M.-C., Lee, Y.J., Kim, T.N. and Cho, S.-J., Sol-gel synthesis and characterization of hydroxyapatite nanorods, Particuology., 7, pp. 466-470, 2009. DOI: 10.1016/j.partic.2009.06.008.
- [5] Sadat-Shojai, M., Khorasani, M.-T., Dinpanah-Khoshdargi, E. and Jamshidi, A., Synthesis methods for nanosized hydroxyapatite with diverse structures., Acta Biomater., 9, pp. 7591-7621, 2013. DOI: 10.1016/j.actbio.2013.04.012.
- [6] Jiang, D. and Zhang, J., Calcium phosphate with well controlled nanostructure for tissue engineering, Curr. Appl. Phys., 9, pp. 252-256, 2009. DOI: 10.1016/j.cap.2009.01.029.
- [7] Gopi, D., Bhuvaneshwari, N., Indira, J., Kanimozhi, K. and Kavitha, L., A novel green template assisted synthesis of hydroxyapatite nanorods and their spectral characterization., Spectrochim. Acta. A.

- Mol. Biomol. Spectrosc., 107, pp. 196-202, 2013. DOI: 10.1016/j.saa.2013.01.052.
- [8] Zhou, R., Si, S. and Zhang, Q., Water-dispersible hydroxyapatite nanoparticles synthesized in aqueous solution containing grape seed extract, *Appl. Surf. Sci.*, 258, pp. 3578-3583, 2012. DOI: 10.1016/j.apsusc.2011.11.119.
- [9] Klinkaewnarong, J., Swatsitang, E., Masingboon, C., Seraphin, S. and Maensiri, S., Synthesis and characterization of nanocrystalline HAP powders prepared by using aloe vera plant extracted solution, *Curr. Appl. Phys.*, 10, pp. 521-525, 2010. DOI: 10.1016/j.cap.2009.07.014.
- [10] Zhu, A., Lu, Y., Si, Y. and Dai, S., Fabricating hydroxyapatite nanorods using a biomacromolecule template, *Appl. Surf. Sci.*, 257, pp. 3174-3179, 2011. DOI: 10.1016/j.apsusc.2010.10.135.
- [11] Sequeda, L.G., Milciades, J., Gutiérrez, S.J., Perdomo, S.J. y Gómez, O.L., Obtención de hidroxiapatita sintética por tres métodos diferentes y su caracterización para ser utilizada como sustituto óseo, *Rev. Colomb. Ciencias Químico-Farmacéuticas*, [en línea]. 2012. Disponible en: <http://www.revistas.unal.edu.co/index.php/rccquifa/article/view/44865/46257>.
- [12] Zhang, X. and Vecchio, K.S., Hydrothermal synthesis of hydroxyapatite rods, *J. Cryst. Growth*, 308, pp. 133-140, 2007. DOI: 10.1016/j.jcrysgro.2007.07.059.
- [13] Liu, Y., Wang, W. and Zhan, Y., A simple route to hydroxyapatite nanofibers, *ELSEVIER*, 56, pp. 496-501, 2002.
- [14] Kamitakahara, M., Takahashi, H. and Ioku, K., Tubular hydroxyapatite formation through a hydrothermal process from α -tricalcium phosphate with anatase, *J. Mater. Sci.*, 47, pp. 4194-4199, 2012. DOI: 10.1007/s10853-012-6274-9.
- [15] Kothapalli, C.R., Wei, M., Legeros, R.Z. and Shaw, M.T., Influence of temperature and aging time on HA synthesized by the hydrothermal method., *J. Mater. Sci. Mater. Med.*, 16, pp. 441-446, 2005. DOI: 10.1007/s10856-005-6984-5.
- [16] Plevin, M., *Encyclopedia of Biophysics*, Springer Berlin Heidelberg, Berlin, Heidelberg, 2013. DOI: 10.1007/978-3-642-16712-6.
- [17] Fahlman, B., *Materials Chemistry*, Springer, Michigan, USA, 2007.
- [18] Patterson, A.L., The scherrer formula for X-ray particle size determination, *Phys. Rev.*, 56, pp. 978-982, 1939. DOI: 10.1103/PhysRev.56.978.
- [19] Wijesinghe, W.P.S.L., Mantilaka, M.M.M.G.P.G., Premalal, E.V.a., Herath, H.M.T.U., Mahalingam, S., Edirisinghe, M., et al., Facile synthesis of both needle-like and spherical hydroxyapatite nanoparticles: Effect of synthetic temperature and calcination on morphology, crystallite size and crystallinity, *Mater. Sci. Eng. C.*, 42, pp. 83-90, 2014. DOI: 10.1016/j.msec.2014.05.032.
- [20] Wan, A.C.A. and Ying, J.Y., Nanomaterials for in situ cell delivery and tissue regeneration, *Adv. Drug Deliv. Rev.*, 62, pp. 731-740, 2010. DOI: 10.1016/j.addr.2010.02.002.
- [21] Giersig, M., *Nanomaterials for application in medicine and biology*, 2007. DOI: 10.1007/978-1-4020-6829-4.
- [22] Tamarinds, USDA Natl. Nutr. Database Stand. Ref. [online]. 2015. Available at: <http://ndb.nal.usda.gov/ndb/foods/show/2436?manu=&fgcd=>;
- [23] Mangos, USDA Natl. Nutr. Database Stand. Ref. [online]. 2015. Available at: <http://ndb.nal.usda.gov/ndb/foods/show/2318?fgcd=&manu=&lfacet=&format=&count=&max=35&offset=&sort=&qlookup=Mango>.
- [24] Grapes american type (slip skin), USDA Natl. Nutr. Database Stand. Ref. [online]. 2015. Available at: <http://ndb.nal.usda.gov/ndb/foods/show/2287?fgcd=&manu=&lfacet=&format=&count=&max=35&offset=&sort=&qlookup=grape>.
- [25] Byrappa, K. and Masahiro, Y., *Handbook of hydrothermal technology: A Technology for Crystal Growth and Materials Processing*, Noyes, New York, 2001.
- [26] Kopp-Alves, A., Bergmann, C.P. and Berutti, F.A., *Novel synthesis and characterization of nanostructured materials*, Springer Berlin Heidelberg, Berlin, Heidelberg, 2013. DOI: 10.1007/978-3-642-41275-2.
- [27] Cao, H., Zhang, L., Zheng, H. and Wang, Z., Hydroxyapatite nanocrystals for biomedical applications, *J. Phys. Chem. C.*, 114, pp. 18352-18357, 2010. DOI: 10.1021/jp106078b.
- [28] Banfield, J.F., Welch, S., Zhang, H., Ebert, T.T. and Penn, R.L., Aggregation-based crystal growth and microstructure development in natural iron oxyhydroxide biomineralization products., *Science*, 289, pp. 751-754, 2000. DOI: 10.1126/science.289.5480.751.
- [29] Medoza-Ruiz, S.C. y Delgado-Mejía, E., Propuesta y evaluación de una síntesis rápida y selectiva de algunos fosfatos de calcio por el método ácido-base, Tesis de grado, Universidad Nacional de Colombia, 2005.
- [30] ASTM INTERNATIONAL, Standard Specification for Composition of Hydroxylapatite for Surgical Implants, 2014. doi: 10.1520/F1185-03R14.2.
- [31] Ossa, C.P.O., Rogero, S.O. and Tschiptschin, a.P., Cytotoxicity study of plasma-sprayed hydroxyapatite coating on high nitrogen austenitic stainless steels., *J. Mater. Sci. Mater. Med.*, 17, pp. 1095-1100, 2006. DOI: 10.1007/s10856-006-0536-5.
- [32] Overgaard, S., Bromose, U., Lind, M., Bünger, C. and Søballe, K., The influence of crystallinity of the hydroxyapatite coating on the fixation of implants. Mechanical and histomorphometric results., *J. Bone Joint Surg. Br.*, 81, pp. 725-731, 1999. DOI: 10.1302/0301-620X.81B4.9282.
- [33] Lee, W.H., Zavgorodniy, A.V., Loo, C.Y. and Rohanizadeh, R., Synthesis and characterization of hydroxyapatite with different crystallinity: Effects on protein adsorption and release, *J. Biomed. Mater. Res.-Part A*, 100 A, pp. 1539-1549, 2012. DOI: 10.1002/jbm.a.34093.
- [34] Yang, Y., Denninson, D. and Ong, J., Protein adsorption and osteoblast precursor cell attachment to hydroxyapatite of different crystallinities, *Oral Maxillofac. Implant.*, 20, pp. 187-192, 2005.
- [35] Koutsopoulos, S., Synthesis and characterization of hydroxyapatite crystals: a review study on the analytical methods., *J. Biomed. Mater. Res.*, 62, pp. 600-612, 2002. DOI: 10.1002/jbm.10280.
- [36] Gopi, D., Bhuvaneshwari, N., Indira, J. and Kavitha, L., Synthesis and spectroscopic investigations of hydroxyapatite using a green chelating agent as template, *Spectrochim. Acta - Part A Mol. Biomol. Spectrosc.*, 104, pp. 292-299, 2013. DOI: 10.1016/j.saa.2012.11.092.
- [37] Gopi, D., Bhuvaneshwari, N., Kavitha, L. and Ramya, S., Novel malic acid mediated green route for the synthesis of hydroxyapatite particles and their spectral characterization, *Ceram. Int.*, 41, pp. 3116-3127, 2015. DOI: 10.1016/j.ceramint.2014.10.156.
- [38] Gopi, D., Kanimozhi, K., Bhuvaneshwari, N., Indira, J. and Kavitha, L., Novel banana peel pectin mediated green route for the synthesis of hydroxyapatite nanoparticles and their spectral characterization, *Spectrochim. Acta - Part A Mol. Biomol. Spectrosc.*, 118, pp. 589-597, 2014. DOI: 10.1016/j.saa.2013.09.034.
- [39] Gopi, D., Bhalaji, P.R., Prakash, V.C.A., Ramasamy, A.K., Kavitha, L. and Ferreira, J.M.F., An effective and facile synthesis of hydroxyapatite powders using oxalic acid-ethylene glycol mixture, *Curr. Appl. Phys.*, 11, pp. 590-593, 2011. DOI: 10.1016/j.cap.2010.10.003.
- [40] Okada, S., Ito, H., Nagai, A., Komotori, J. and Imai, H., Adhesion of osteoblast-like cells on nanostructured hydroxyapatite., *Acta Biomater.*, 6, pp. 591-597, 2010. DOI: 10.1016/j.actbio.2009.07.037.
- [41] Webster, T.J., Ergun, C., Doremus, R.H., Siegel, R.W. and Bizios, R., Enhanced functions of osteoblasts on nanophase ceramics., *Biomaterials*, [online]. 21, pp. 1803-1810, 2000. Available at: <http://www.ncbi.nlm.nih.gov/pubmed/10905463>.
- [42] Webster, T.J., Ergun, C., Doremus, R.H., Siegel, R.W. and Bizios, R., Enhanced osteoclast-like cell functions on nanophase ceramics., *Biomaterials*, [online]. 22, pp. 1327-1333, 2001. Available at: <http://www.ncbi.nlm.nih.gov/pubmed/11336305>.
- [43] Walmsley, G.G., McArdle, A., Tevlin, R., Momeni, A., Atashroo, D., Hu, M.S., et al., Nanotechnology in bone tissue engineering, *Nanomedicine Nanotechnology, Biol. Med.*, 1(5), pp. 1253-1263, 2015. DOI: 10.1016/j.nano.2015.02.013.

M. Buitrago-Vásquez, received the BSc. Bioengineer in 2014 and the MSc Materials Engineering in 2017, both from Universidad de Antioquia, Medellín, Colombia, she is researcher of Grupo de Investigación en Biomateriales. Her research interests include biomaterials, composite biomaterials, calcium phosphates and biopolymers.
ORCID: 0000-0002-7616-0532.

C.P Ossa-Orozco, received the BSc. Eng in Mining and Metallurgy Engineering in 2000, from Universidad Nacional de Colombia, Medellín, Colombia and the PhD degree in Materials and Metallurgy in 2005, from Universidade de São Paulo, São Paulo, Brazil. Actually is associate professor of Universidad de Antioquia and researcher of Grupo de Investigación en Biomateriales. Her research interests include synthesis and characterization of biomaterials, scaffolds, calcium phosphates and natural polymers.
ORCID: 0000-0002-0223-4113